NASA/TM–2019-220249

A Simple Transient Thermal Test Assembly for Insulation Materials

Kamran Daryabeigi
Langley Research Center, Hampton, Virginia

Max L.Blosser
Max Blosser Consulting, Williamsburg, Virginia

Wayne D. Geouge
Langley Research Center, Hampton, Virginia

Jonathan S. Cheatwood
Virginia Polytechnic Institute and State University, Blacksburg, Virginia

February 2019

NASA STI Program . . . in Profile

Since its founding, NASA has been dedicated to the advancement of aeronautics and space science. The NASA scientific and technical information (STI) program plays a key part in helping NASA maintain this important role.

The NASA STI program operates under the auspices of the Agency Chief Information Officer. It collects, organizes, provides for archiving, and disseminates NASA's STI. The NASA STI program provides access to the NTRS Registered and its public interface, the NASA Technical Reports Server, thus providing one of the largest collections of aeronautical and space science STI in the world. Results are published in both non-NASA channels and by NASA in the NASA STI Report Series, which includes the following report types:

- TECHNICAL PUBLICATION. Reports of completed research or a major significant phase of research that present the results of NASA Programs and include extensive data or theoretical analysis. Includes compilations of significant scientific and technical data and information deemed to be of continuing reference value. NASA counter-part of peer-reviewed formal professional papers but has less stringent limitations on manuscript length and extent of graphic presentations.

- TECHNICAL MEMORANDUM. Scientific and technical findings that are preliminary or of specialized interest, e.g., quick release reports, working papers, and bibliographies that contain minimal annotation. Does not contain extensive analysis.

- CONTRACTOR REPORT. Scientific and technical findings by NASA-sponsored contractors and grantees.

- CONFERENCE PUBLICATION. Collected papers from scientific and technical conferences, symposia, seminars, or other meetings sponsored or co-sponsored by NASA.

- SPECIAL PUBLICATION. Scientific, technical, or historical information from NASA programs, projects, and missions, often concerned with subjects having substantial public interest.

- TECHNICAL TRANSLATION. English-language translations of foreign scientific and technical material pertinent to NASA's mission.

Specialized services also include organizing and publishing research results, distributing specialized research announcements and feeds, providing information desk and personal search support, and enabling data exchange services.

For more information about the NASA STI program, see the following:

- Access the NASA STI program home page at http://www.sti.nasa.gov

- E-mail your question to help@sti.nasa.gov

- Phone the NASA STI Information Desk at 757-864-9658

- Write to:
  NASA STI Information Desk
  Mail Stop 148
  NASA Langley Research Center
  Hampton, VA 23681-2199

NASA/TM–2019-220249

A Simple Transient Thermal Test Assembly for Insulation Materials

Kamran Daryabeigi
Langley Research Center, Hampton, Virginia

Max L. Blosser
Max Blosser Consulting, Williamsburg, Virginia

Jonathan S. Cheatwood
Virginia Polytechnic Institute and State University, Blacksburg, Virginia

National Aeronautics and
Space Administration

Langley Research Center
Hampton, Virginia 23681-2199

February 2019

Acknowledgments

The authors are grateful to Mr. John M. Wells (Northrop Grumman) for his assistance with the data acquisition system for the tests.

Available from:

NASA STI Program / Mail Stop 148
NASA Langley Research Center
Hampton, VA 23681-2199
Fax: 757-864-6500

Contents

List of Figures

List of Tables

Nomenclature

APA	**A**lumina **pa**per
ISO	**I**nternational **O**rganization of **S**tandardization
RMS	**R**oot **m**ean **s**quare
THERMIC	**Therm**al **i**nsulation **c**haracterization

List of Symbols

S_i	Temperature for thermocouples on Inconel septum plate (i = 1, 4)
S_{avg}	Average temperature of septum plate thermocouples (S_1, S_2, S_3)
t	Time
T	Temperature
Tc_k	Temperature for thermocouples installed between APA layers (k = 1, 3)
Ti_j	Temperature for thermocouples on titanium witness plate (j = 21, 25)
Ti_{cen}	Average temperature of thermocouples in the central region of titanium witness plate (Ti_{21} , Ti_{22} , Ti_{23})
Ti_{edge}	Average temperature of thermocouples in the outer region of titanium witness plate (Ti_{24} , Ti_{25})
ΔT	Temperature difference

Abstract

A simple transient thermal test was developed for evaluating the thermal performance of high-temperature flexible insulation materials in atmospheric pressure air. The test setup was inspired by the test assembly used for evaluating the performance of fire shelters and fire protective clothing. The heating source used was a burner supplied with propane gas that can generate relatively uniform heating over a wide area. The ratio of the in-plane width to thickness of the insulation test sample in the test assembly was selected to be greater than ten so that the heat transfer in the center of the test assembly was nearly one-dimensional. A rigid, thin Inconel plate was used as the septum plate directly exposed to the flame to provide a relatively uniform, known-temperature boundary condition for the test assembly, and to prevent convective heat transfer through the test insulation from the burner. The test sample, flexible alumina paper insulation, was placed between the Inconel plate and a thin titanium witness plate. The overall assembly was further insulated using a combination of rigid and flexible ceramic insulations to minimize heat losses from the periphery of the test assembly. Thermocouples installed on the septum and witness plates and inside the insulation test sample provided temperature measurements at various locations. For the evaluation tests, the Inconel septum plate reached temperatures between 780˚C and 850˚C for tests with flame exposure durations of 120 sec to 300 sec. The measured temperatures for various tests with similar flame exposure times were repeatable. A one-dimensional numerical heat transfer model of the test assembly was developed. The close agreement between measured and predicted temperatures on the titanium witness plate and inside the insulation test sample indicated that this test may provide a one-dimensional thermal testing capability for evaluation of thermal performance of similar insulations.

Introduction

There is a need for a simple test for quick turnaround thermal performance evaluation testing of novel high-temperature insulations that are being developed. The test described in this paper is intended for comparison of thermal performance of various insulations. The test, combined with a numerical thermal model of the test configuration, has also the potential to be used for estimation of unknown thermal properties of insulation samples. There are standard steady-state techniques (Refs. 1, 2) for measuring thermal conductivity of high-porosity, low-density thermal insulations, but they require significant setup and test time to achieve steady-state conditions in order to yield accurate results. Because of the high porosity of these insulations, typically larger than 90 percent, the thermal conductivity of these insulations are a function of not only temperature, but the environmental pressure and gaseous medium (Ref. 3). For a quick turnaround system, having the test assembly operate at atmospheric pressure air to avoid complexities involved with testing in a vacuum chamber or in an inert environment is desirable. Furthermore, imposing a constant, spatially uniform heat flux on the hot side of the system is also desirable. Moreover, the test sample should have a large ratio of width to thickness to reduce the influence of the edge effects and thus result in nearly one dimensional (1-D) heat transfer through the thickness in the center of the test assembly. Preventing any forced convective flow from the burner through the test sample is also important, because such flow will not be present in most applications using the insulations, nor in the more

rigorous steady-state thermal conductivity measurement test techniques for characterizing thermal conductivity of insulations. Standard techniques for measurement of specific heat can be utilized for determining the specific heat of the insulation sample (Ref. 4), therefore, determination of the insulation sample specific heat was outside the scope of the present study.

The International Organization of Standardization (ISO) standard 9151 (Ref. 5) for testing heat transmission in protective clothing against heat and flame is a simple test assembly that has most of the desired features required in this study. This standard uses a flat topped Meker™ burner with propane gas as the working medium, and provides a spatially uniform heat flux over an extended area. The Meker burner's flame structure is an aggregate of small cones, rather than one large cone as in a Bunsen burner, and the heating from the Meker burner is distributed more evenly across the test sample surface (Ref. 6). The ISO 9151 uses a 150 mm by 150 mm wide, 1.6 mm-thick copper plate as the specimen support frame, with a 50 mm by 50 mm hole in the center of the plate. This support frame gets exposed to the flame from the Meker burner. The test sample for ISO 9151 standard, 150 mm by 150 mm wide, is sandwiched between this support frame and a calorimeter location plate. The calorimeter location plate is a 149 mm by 149 mm wide, 6 mm-thick aluminum plate with a 90 mm circular hole located in the center of the plate. A copper disk calorimeter is located in the central hole of the calorimeter location plate. A support stand is used to locate the specimen support frame 50 mm above the top face of the Meker burner. Testing consists of exposing the test assembly to a heat flux of 8 W/cm^2, and determining heat transmission through the test sample by measuring the time required for the copper calorimeter temperature to rise by 24°C. NASA Langley Research Center (LaRC) has recently used the ISO 9151 standard setup and variations of this setup for evaluation of the thermal performance of various proposed layups for fire shelters for wildland firefighters (Ref. 6).

This ISO 9151 test assembly is an efficient, quick turnaround test assembly for evaluating performance of protective clothing and fire shelter layups, but has some shortcomings for the intended purposes of this investigation. Only the central 50 mm by 50 mm area of the test sample front surface is directly exposed to the flame, while the rest of the test sample front face is located behind the copper specimen support frame; therefore, the front face of the test sample is not exposed to spatially uniform heating conditions. Furthermore, there is no insulation around the periphery of the test setup to minimize lateral heat losses. The combination of these two effects could results in deviations from 1-D heat transfer through thicker test samples in the through thickness direction. Furthermore, since part of the test sample front face is directly exposed to the flame though the center hole of the specimen support frame, there is possibility of forced convective heat transfer through the test sample from the burner.

The test assembly adopted in this investigation was inspired by the ISO 9151 standard, but included some modifications to make the test assembly more suitable for the intended use of testing and characterization of high-temperature flexible insulations. The main modification consisted of using a rigid specimen support frame (septum plate) without any holes to prevent convective flow through the test assembly, and to provide a more spatially uniform temperature boundary condition for the insulation test sample. The other modification was using rigid insulation boards around the periphery of the test sample to minimize lateral heat losses. The last modification was to use a rigid witness plate without any holes instead of the calorimeter plate, and placing additional insulation on top of this witness plate. The temperature rise of this witness plate can be used for comparing thermal performance of various insulations. The overall objective was to develop a 1-D test assembly that could be used for testing and comparison of thermal performance of various flexible insulations. The description of the test assembly is provided in the forthcoming sections. Results of multiple tests on a flexible insulation with well-established thermal properties are provided to determine the repeatability of the test setup. Then, the test results are compared with 1-D numerical heat transfer model predictions of the test assembly, to assess whether thermal performance of the test assembly matches the thermal model predictions. Close agreement between test results and model predictions would indicate a properly designed 1-D thermal test. Even though the main emphasis of the present study is on developing a test bed for flexible insulations, rigid insulations can also

be tested as long as thermal contact resistance between the rigid insulation and rigid surrounding plates are accounted for (Ref. 7). This newly developed test was named the **therm**al **i**nsulation **c**haracterization (THERMIC) test.

Test Assembly

A sketch of the THERMIC test assembly is shown in Fig. 1. The major components of the test assembly from bottom to top were the Meker burner, test assembly holder (not shown in the sketch), Inconel septum plate, insulation test sample, titanium witness plate, additional flexible insulation, and a rigid insulation board. The entire assembly was surrounded by rigid insulation board picture frames as shown in the sketch. Different components are subsequently described.

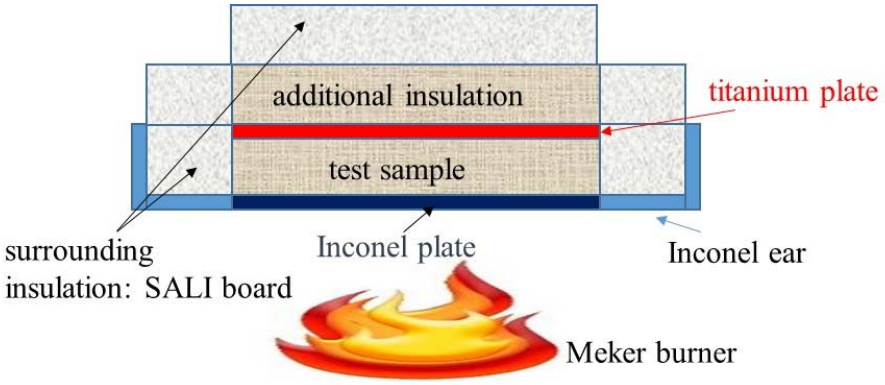

Figure 1. Sketch of THERMIC test assembly

The stainless steel test assembly holder plate is shown in Fig. 2a. This holder plate was bolted to a support structure assembly on one end, while the other end with the wide opening in the middle was used for the placement of the THERMIC test assembly. A photograph of the holder plate in the test assembly is shown in Fig. 2b.

A 2.54-mm thick Inconel plate, 152 mm by 152 mm wide was used as the septum plate, placed on top of the test assembly holder plate and directly exposed to the flame. Inconel is a high-temperature nickel alloy that can withstand temperatures as high as 1100°C in air with minimum levels of oxidation, and has a moderate value of thermal conductivity (around 10 W/m.K at room temperature) to provide a spatially uniform temperature boundary condition. Three slits were machined along the periphery of the septum plate along each side, with slit spacing of 38.1 mm. The slits were approximately two mm wide and 22 mm long, and were used to minimize bowing of the plate when exposed to rapid heating. The septum plate had two 12.7 mm wide and 50.8 mm long ears on each side. The ears were bent at their mid-length to locate and retain the rigid insulation board that surrounds the test assembly located on top of the septum plate. A photograph of the septum plate with the slits and unbent ears is shown in Fig. 3a. The plate was heat treated in an oven at 900˚C for three one-hour long exposures to achieve stable oxidation of the plate, with an effective emittance/absorptance of 0.80 or higher. A photograph of the plate after heat treatment is shown in Fig. 3b. Grooves that are observable in the image were intended for installation and routing of thermocouples and will be discussed in the instrumentation section. The Inconel septum plate with bent ears was placed on the holder plate in the test assembly as shown in Fig. 2b.

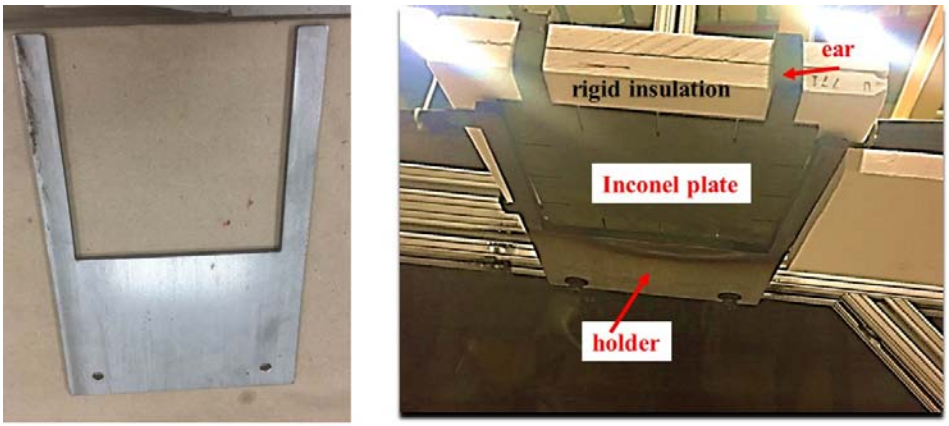

Figure 2. Test assembly holder plate: a) stand alone, b) installed in THERMIC

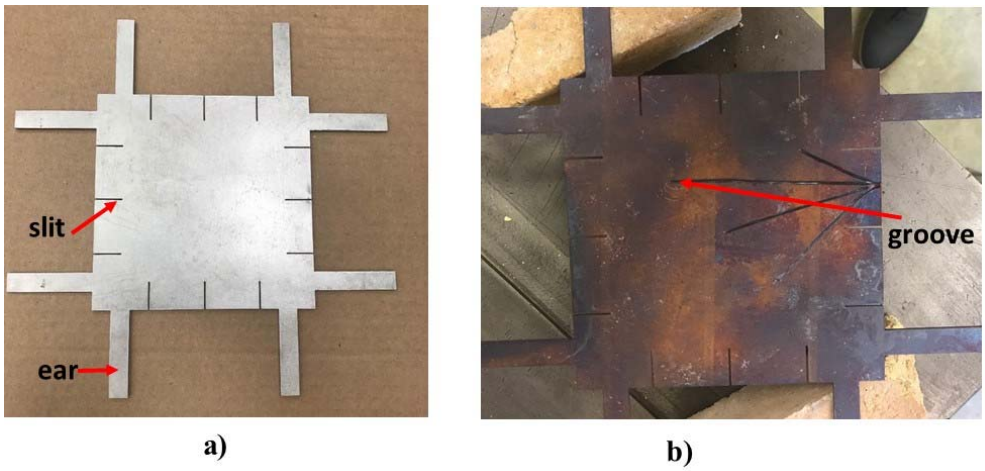

Figure 3. Inconel septum plate a) prior to heat treatment, b) post heat treatment

Rigid insulation board picture frames, 25.4 mm wide with outer dimensions of 203.2 mm were placed on the septum plate, to provide additional insulation capability around the perimeter of the entire test assembly, as shown in Fig. 2b. Two 12.7-mm thick SALI™ rigid boards made of polycrystalline alumina fibers bound in a mullite binder matrix were used. The insulation test sample, titanium witness plate, and additional flexible insulation were installed inside the insulation board picture frames and on top of the Inconel septum plate. A photograph of the rigid insulation board picture frames used in THERMIC is shown in Fig. 4. The metallic plate shown in the photograph is the titanium witness plate which will be described in the upcoming discussions.

A 152 mm by 152 mm wide insulation test sample was placed inside the rigid picture frame and on top of the Inconel septum plate. As a means to approximately achieve 1-D heat transfer in the center of the sample, a test sample width to thickness ratio of ten is desired. Thus, the total insulation test sample thickness should not exceed 15.2 mm. The insulation test sample used in the present study consisted of thin insulation felt layers, where multiple layers had to be stacked to achieve the desired total thickness.

This allowed installation of thermocouples in between felt layers for through-thickness temperature measurements during the test. The flexible insulation chosen was alumina paper insulation (APA™) which has well-established thermal properties (Ref. 3). APA is a thin, paper-like structure made of polycrystalline alumina fibers, which is composed of 86 percent alumina, ten percent silica, and four percent other oxides. The actual layer thickness once installed in the assembly was determined to be 1.16 mm, resulting in total thickness of 11.6 mm for a 10-layer layup. The effective density of the test sample was 98.2 kg/m^3, with an effective porosity of 97.1 percent. A photograph of six layers of the APA test sample is shown in Fig. 5.

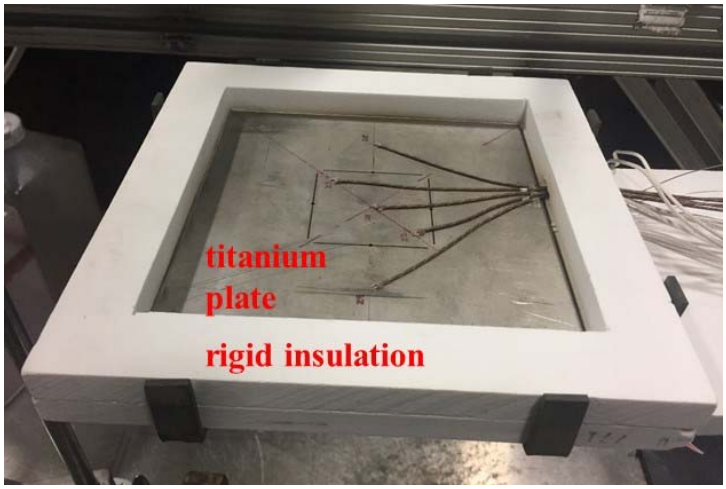

Figure 4. Rigid insulation board picture frames in test assembly

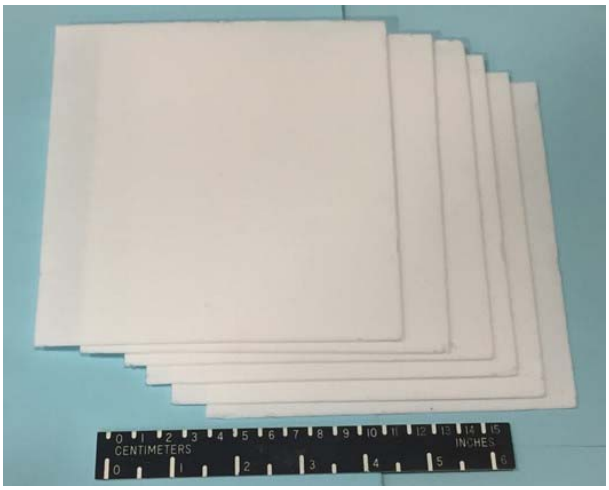

Figure 5. APA insulation test sample (6 layers shown)

A 1.965-mm thick titanium plate, 150 mm by 150 mm wide was used as the witness plate and placed on top of the insulation test sample. The titanium plate used was Ti-6Al-4V, which has six percent aluminum and four percent vanadium. A photograph of the titanium plate is shown in Fig. 6a. The titanium plate was slightly undersized, 150 mm compared to 152 mm for other components, to avoid direct contact with the rigid insulation board picture frame. This lack of direct contact would eliminate a direct solid conduction path from the titanium plate to the rigid insulation board. Four slits, 0.38 mm wide and 45.7 mm long, were made in the titanium plate as shown in the figure. The four slits formed a partial square with 50.8 mm sides,

but with the corners missing. The purpose of these slits was to thermally isolate the central 50.8 mm by 50.8 mm section of the titanium plate from the outer section of the titanium plate. Higher temperatures at the center of the test assembly compared to the edges were expected throughout the entire layup, including the titanium plate. By incorporating the slits, the cross sectional area for thermal conduction through the titanium plate from the outer to central section was significantly reduced, thus providing some thermal isolation of the cooler outer section from the warmer central section. This technique of incorporating thin slits in witness plates to isolate edge effects has been previously used in other studies (Ref. 8). One side of the titanium plate, the side facing the test sample, was coated with an optically flat black paint with an effective emittance value exceeding 0.85, as seen in Fig. 6b. The other side of the titanium plate was not painted.

Additional 152 mm by 152 mm wide insulation layers were placed on top of the titanium witness plate, inside the second rigid picture frame. This additional insulation also consisted of ten APA layers, stacked to achieve a total thickness of 11.6 mm. A 152 mm by 152 mm wide, 12.7 mm thick rigid insulation board

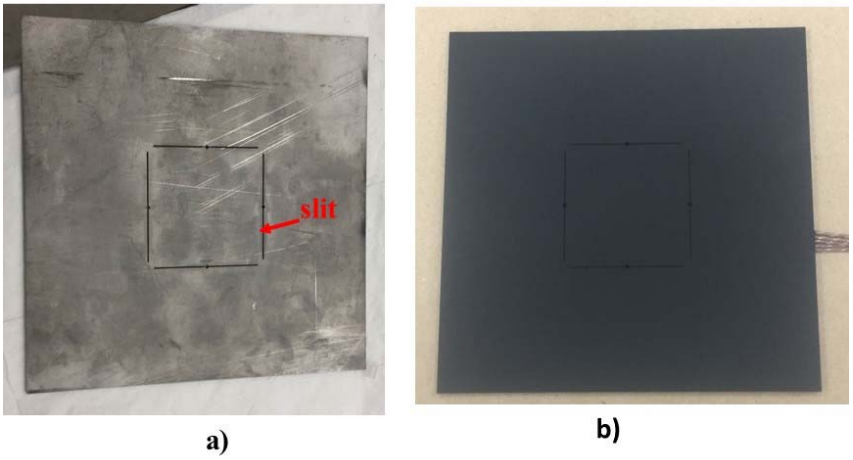

Figure 6. Photograph of titanium witness plate: a) top side, b) bottom side

was placed on top of the additional flexible insulation to further minimize heat losses from the top side of the assembly.

Thermal Instrumentation

The Inconel septum plate was instrumented with four metal sheathed type K thermocouples with sheath outside diameters of 0.51mm and grounded junctions. Thin grooves, 0.63 mm wide and deep were made in the septum plate to route the thermocouple leads and ensure that the leads were flush mounted with the plate surface as shown in Fig. 3b. A photograph of the thermocouples installed inside the grooves is shown in Fig. 7a. Thin stainless steel strips were spot welded to the Inconel plate along each thermocouple lead to hold the thermocouple in the groove. One thermocouple was placed at the center of the plate, and designated as S_1. Two other thermocouples were installed along the plate diagonal, approximately 35.4 mm away from the plate center on either side of the center, and designated as S_2 and S_3. One more thermocouple was installed along the other diagonal, 53.2 mm away from the plate center, and designated as S_4. The average of the temperature data for thermocouples S_1, S_2, and S_3, designated as S_{avg}, was used as one boundary condition for the thermal analysis. Thermocouple S_4 was located close to one corner of the septum plate, so this thermocouple's readings were suspected to be lower than the other three thermocouples. Data from this thermocouple served to provide information on septum plate temperature non-uniformity near the corners.

Five type K thermocouples with wire diameter of 0.25 mm with fiberglass insulation were installed on the top side of the titanium witness plate, the unpainted side that was adjacent to the additional flexible insulation. A photograph of the top side of the titanium witness plate with the installed thermocouples is shown in Fig. 7b. The thermocouple beads were spot welded to the titanium witness plate, and thin stainless steel straps welded to the plate at the plate edge were used to hold the thermocouple wires to the plate. Three of the thermocouples were installed in the central 50.8 mm by 50.8 mm section of the plate surrounded by the slits. These thermocouples were installed along the plate diagonal, with thermocouple designated as Ti_{21} located at the center, and the other two thermocouples 22.9 mm away from the center on either side of the center, and designated as Ti_{22} and Ti_{23}. Two additional thermocouples were installed on the titanium witness plate outer section, halfway between the slits and plate edges, and designated as Ti_{24} and Ti_{25}. The average of temperature readings for thermocouples Ti_{21}, Ti_{22}, and Ti_{23}, designated as Ti_{cen}, was used as the titanium witness plate center section temperature, while the average of the other two thermocouples, designated as Ti_{edge}, was used as the titanium witness plate edge section temperature.

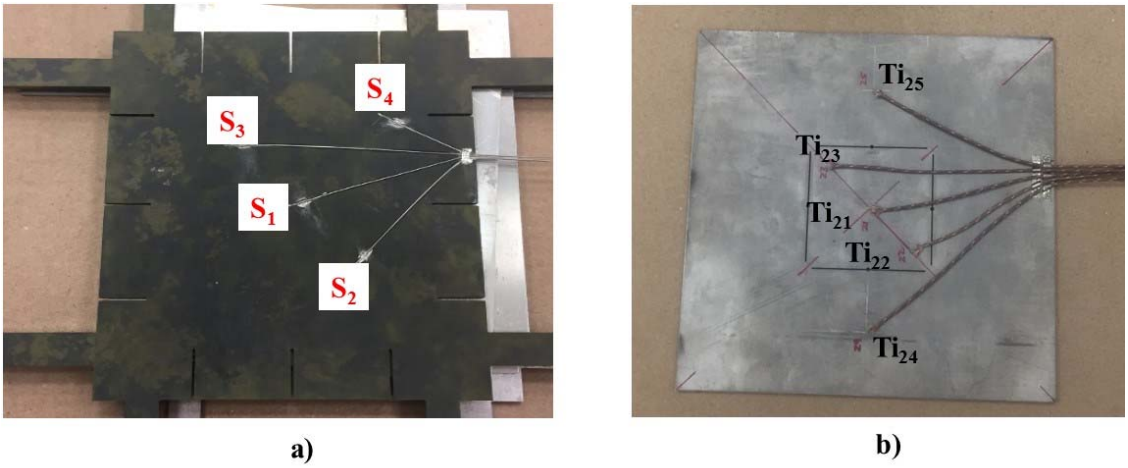

Figure 7. Photograph of thermocouples on metallic plates: a) Inconel, b) titanium

Three specialty-made foil thermocouples were used for measuring temperatures between insulation layers. These thermocouples consisted of bare Type K thermocouple leads welded to a 6.35 mm by 6.35 mm wide, 0.254 mm thick Inconel foil. The foil acted as the effective junction area for the thermocouple. Use of extended area thermocouple junctions is advantageous in high porosity insulations where radiation heat transfer can be an important mode of heat transfer. A photograph of a foil thermocouple is shown in Fig. 8a. The length of the thermocouple leads located between the insulations layers was bare wire, to minimize thermal disturbance in the test sample. The remainder of the length of the leads was installed in Nextel™ sleeving to provide electrical isolation. These foil thermocouples were installed in the sample during assembly of test hardware in such a way to ensure that the bare lead wires between insulation layers were routed far enough from each other to prevent direct electrical contact between them. A photograph of the foil thermocouple installed on top of one APA layer in the additional flexible insulation is shown in Fig. 8b. Two of these foil thermocouples were installed inside the test sample. For the APA test sample with 10 layers of APA between the Inconel septum and titanium witness plates, foil thermocouples were placed on top of the fifth and second APA layers from the titanium witness plate, and labeled as Tc_1 and Tc_2. Since each APA layer is 1.17 mm thick, the distances between these two foil thermocouples and titanium witness plate were 5.84 mm and 2.34 mm, respectively. One foil thermocouple was installed on top of the fourth layer of APA from the titanium witness plate inside the additional flexible insulation. The distance between this thermocouple and titanium witness plate was 4.67 mm. This thermocouple was designated as Tc_3 and the temperature data from Tc_3 could either serve as one boundary condition for the

thermal analysis model, or for an additional check of the thermal model inside the additional flexible insulation. Thermocouple designations for various thermocouples are provided in Table 1.

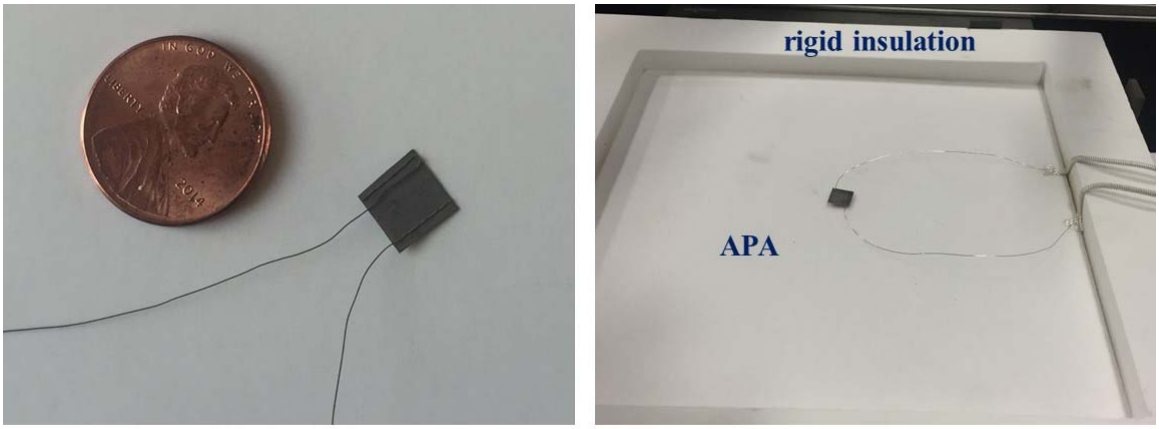

a) b)

Figure 8. Foil thermocouple: a) as fabricated, b) installed on APA layer

Table 1. Thermocouple designations

Region	Thermocouples	Average Values
Inconel plate	S_1, S_2, S_3, S_4	S_{avg}: Average of S_1, S_2, S_3
Test sample	Tc_1, Tc_2	-----
Titanium plate	Ti_{21}, Ti_{22}, Ti_{23}, Ti_{24}, Ti_{25}	Ti_{cen}: Average of Ti_{21}, Ti_{22}, Ti_{23} Ti_{edge}: Average of Ti_{24}, Ti_{25}
Additional Insulation	Tc_3	-----

Test Procedure

The test procedure consisted of turning the Meker burner flame on and establishing a desired propane gas flow rate, placing the Meker burner under the test assembly for the desired test duration, and then removing the burner and terminating the flame. The Meker burner was installed on a swivel mechanism, which allowed for easy movement between two locations: park position, and test assembly position. The Meker burner flame was turned on, and the desired propane gas flow rate was established while the Meker burner was in the park position. Then, the Meker burner was rotated and placed under the THERMIC test assembly for the desired flame exposure duration. Five tests are reported here. For the first three tests, the flame exposure duration was 180 seconds, while the fourth and fifth tests had flame exposure durations of 120 and 300 seconds, respectively. At the end of the desired flame exposure duration, the Meker burner was rotated and placed in the park position before the gas flow was turned off. Thermocouple data was collected for an additional 120 seconds (approximately) after removing the burner, to obtain cool-down data.

Thermal Model

A transient 1-D finite difference thermal model with a Crank-Nicolson implicit time marching technique (Ref. 9) written in Fortran programming language was used to model heat transfer in the THERMIC test assembly. The domain of the analysis consisted of APA test sample, titanium witness plate, and the additional flexible insulation. A convergence study was conducted which found that using 22 nodes across the 10-layer APA test sample was sufficient to obtain an accurate numerical solution of temperature distributions throughout the test sample. S_{avg}, which was representative of temperature at the interface of the Inconel septum plate and APA test sample, was used as the specified temperature boundary condition on the hot side (bottom). An adiabatic boundary condition was assumed at the interface of the additional flexible insulation and rigid insulation on the cold side (top). Another option would have been to use the measured temperature of the foil thermocouple Tc_3 located in the additional flexible insulation as the specified temperature boundary condition on the cold side. The thermal properties used for APA are provided in Table 2. The thermal conductivity data for APA at atmospheric pressure as a function of temperature were obtained from data in Ref. 3. The specific heat for APA was assumed to be that of pure alumina and obtained from Ref. 10. The APA density was 98.2 kg/m^3 as determined from mass and dimension measurements of ten layers of the test sample. The thermal conductivity and specific heat of Ti-6Al-4V are listed in Table 3, and were obtained from Ref. 11.

A time step increment of one second was used for the numerical solution of the heat transfer equations, which matched the test data acquisition rate. The comparison of measured and predicted temperatures at Ti_{cen}, Tc_1, and Tc_2 was used to evaluate the test assembly thermal performance. Close agreement between measured and predicted data would indicate that the heat transfer in the test assembly was 1-D, and that THERMIC can be a satisfactory test bed for testing similar insulations. The presence of thermocouples in the test sample and on various plates was ignored in the thermal model. The primary measure of comparison was Ti_{cen}. The titanium plate had high volumetric heat capacity so that the volumetric heat capacity of the thermocouples installed on the plate could be ignored without significantly affecting comparison of the test and numerical model at the plate location. The volumetric heat capacity of the foil thermocouples installed between insulation layers could affect transient temperature results at these locations, and ignoring them in the numerical model could affect comparison of test and model predictions at these locations.

Table 2. APA thermal properties

T (K)	c_p (J/kg.K)	k (W/m.K)	T (K)	c_p (J/kg.K)	k (W/m.K)
300	788.6	0.0306	1000	1224.4	0.1252
400	922.4	0.0402	1100	1238.6	0.1477
500	1019.4	0.0505	1200	1248.8	0.1741
600	1089.8	0.0618	1300	1256.3	0.2052
700	1140.9	0.0745	1400	1261.7	0.242
800	1178.0	0.0891	1500	1265.6	0.2857
900	1204.9	0.1058			

Table 3. Ti-6Al-4V thermal properties

T (K)	c_p (J/kg.K)	k (W/m.K)
255.6	523.4	6.92
366.7	569.4	7.44
477.8	577.8	8.66
588.9	602.9	10.39
700.0	640.6	11.94
811.1	699.2	13.67
922.2	762.0	14.89

Discussion of Results

A photograph of the THERMIC test assembly during testing is shown in Fig. 9. The flame from the Meker burner is seen impinging on the Inconel septum plate. A summary of pertinent test information for the five tests reported is included in Table 4. The information includes test number and flame exposure duration, which varied between 120 and 300 seconds. The reported test number starts with 9, because the initial eight tests were preliminary tests used to trouble shoot and fine tune the test assembly and test procedure. For each test the temperature data for the test assembly were recorded for at least another 120 seconds after removal of flame from the test assembly to monitor the cool-down. The total test time listed in the table was the sum of the flame exposure duration and recorded cool-down duration for each test. For example, test 1 had a nominal 180 second flame exposure duration, and a 185 second cool-down duration, for a total test duration of 365 seconds. The maximum S_{avg} value achieved during each test is also listed in the table. The maximum S_{avg} was 780˚C for the 120-second flame exposure test (test 12), and varied between 835˚C and 847˚C for the other four tests. The average initial Ti_{cen} are also listed in the table and varied between 20.9˚C and 22.5˚C.

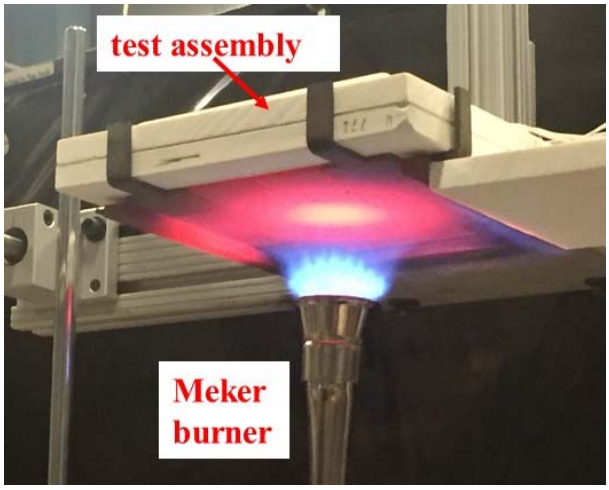

Figure 9. THERMIC test assembly during test

Table 4. Test information

Test Number	Flame exposure duration (sec)	Total test duration (sec)	Maximum Inconel plate temperature, S_{avg}, (˚C)	Initial titanium plate temperature, Ti_{cen}, (˚C)
9	180	365	839	21.9
10	180	346	835	22.2
11	180	371	842	22
12	120	244	780	20.9
13	300	443	847	22.5

The measured temperature distributions for test 9 are provided in Fig. 10. The data shown are S_{avg}, Tc_1, Tc_2, Ti_{cen} , Ti_{edeg}, and Tc_3. The temperature distributions followed expected patterns with temperature levels decreasing as distance from the Inconel septum plate increased. The delay in temperature rise also increased with increasing distance from the septum plate, and Ti_{cen} was slightly higher than the Ti_{edge}, as expected. The Inconel septum plate thermocouple data for test 9 is presented in Fig. 11. The temperature in the middle of the plate, S_1, was the highest, and temperature at the corner of the plate, S_4, was the lowest. The other two thermocouples S_2 and S_3 had readings that were similar, and were between S_1 and S_4 thermocouple readings. The titanium witness plate thermocouple data for test 9 is presented in Fig. 12. The three thermocouples in the middle of the plate, Ti_1, Ti_2, and Ti_3, had readings that were close to each other, and were higher than the edge thermocouples, Ti_4 and Ti_5. To investigate the spatial non-uniformity of temperatures

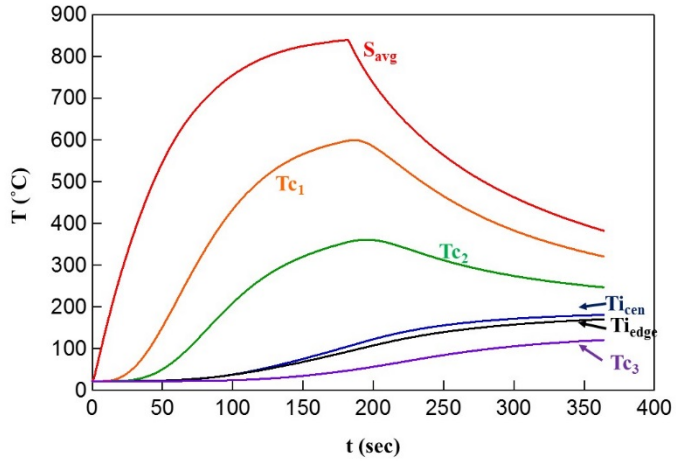

Figure 10. Test 9 temperature data

in these regions (septum average, titanium center, and titanium edge), the ratio of standard deviation to average temperature in each region at each time was calculated and presented in Fig. 13. For the septum plate the spatial temperature non uniformity varied between 14% and 4% during flame exposure, with non-uniformity decreasing with increasing test time. The spatial temperature non uniformities were less than 4% and 2 % for Ti_{edge} and Ti_{cen}, respectively. These observed patterns were typical for all the tests.

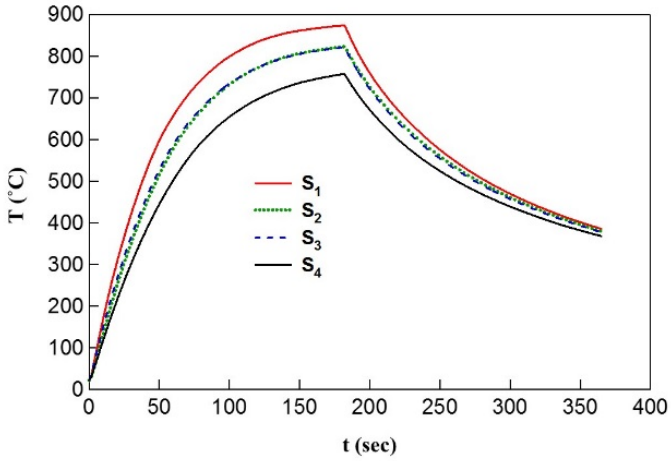

Figure 11. Inconel septum plate temperatures for test 9

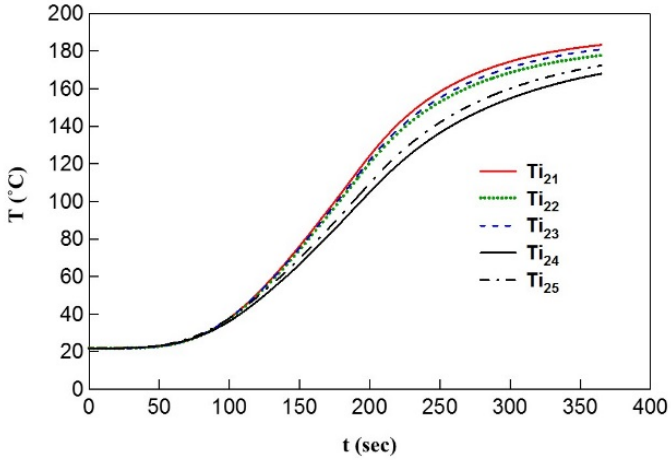

Figure 12. Titanium witness plate temperatures for test 9

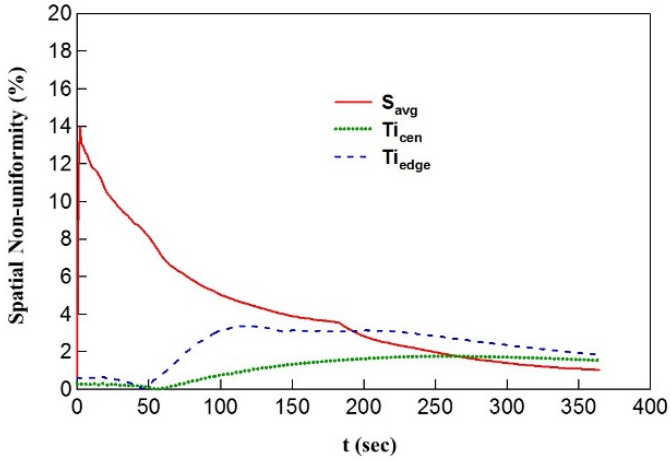

Figure 13. Spatial temperature non-uniformity for test 9

To investigate test repeatability, temperature data from tests 9, 10, and 11, the three tests with 180 second flame exposure duration are shown in Fig. 14. Comparison of temperature data for S_{avg}, Tc_2, and Ti_{cen} are

provided in Fig. 14.a, while data for Tc_1, Ti_{edge}, and Tc_3 are shown in Fig. 14.b. Color coding is used to indicate different thermocouple data in each graph, while the different line styles are used to indicate different test numbers: solid line for test 9, dotted line for test 10, and dashed line for test 11. The tests appeared to be repeatable. The standard deviation of temperature variations for the three tests at various thermocouple locations is provided in Fig. 15a. The maximum variation was 10°C, 8°C, and 5°C for S_{avg}, Tc_1, and Tc_2, respectively. The maximum variations were less than 3°C for Tc_3 and Ti_{cen}. The relative repeatability was evaluated by obtaining the ratio of standard deviation between tests to average temperature for the three tests at each instant of time and is presented in Fig. 15b. The relative repeatability was less than or equal to 4% for Tc_1 and Tc_2, and less than 2% for Ti_{cen} and Tc_3, and less than 4% for S_{avg} after 30 seconds into the test. Considering the simple nature of the test assembly and tests, and the simple test control protocol used, the repeatability of test results was exceptional.

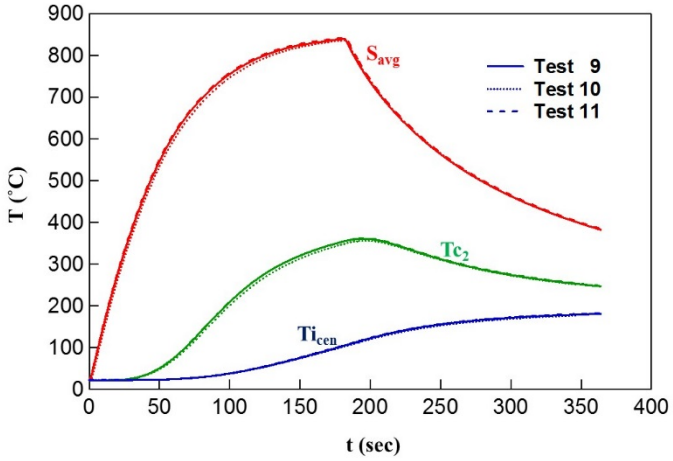

a)

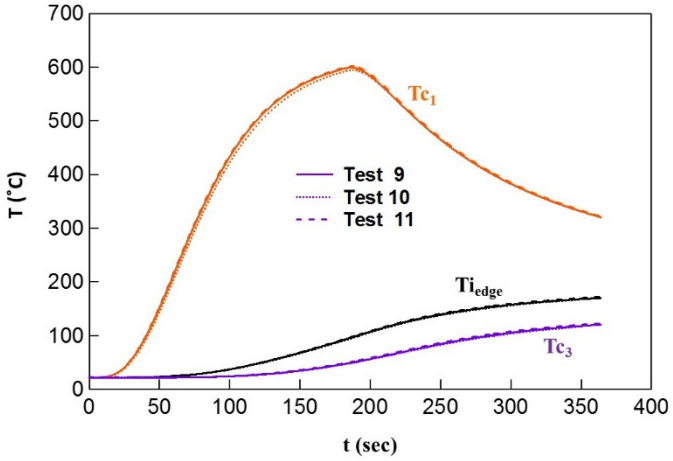

b)

Figure 14. Comparison of temperature data for tests 9 through 11: a) S_{avg}, Tc_2, and Ti_{cen}, b) Tc_2, Ti_{edge}, and Tc_3

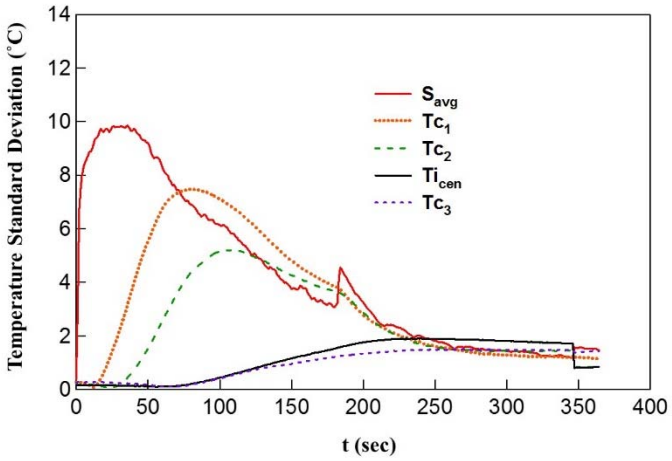

a)

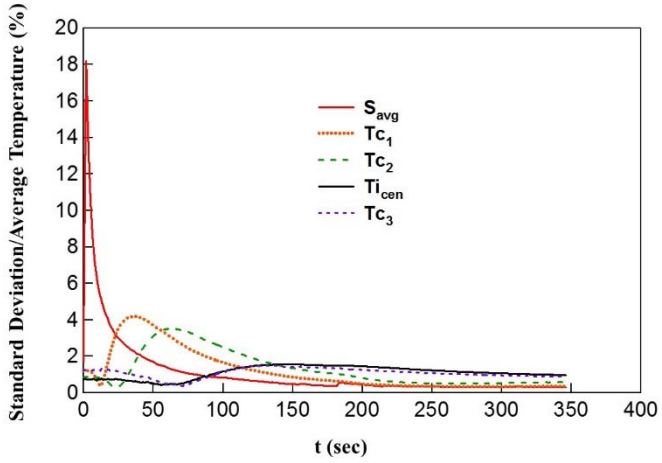

b)

Figure 15. Temperature repeatability for tests 9 through 11: a) standard deviation, b) standard deviation/average temperature

The comparison of test data and the numerical heat transfer model predictions for Tc_1, Tc_2 and Ti_{cen} for test 9 is provided in Fig. 16. The model predictions are displayed with solid lines, while measurements are presented with dashed lines. For the two embedded thermocouples in the test sample, the predictions rose at a faster rate than the measurements up to 100 seconds, then the predictions were lower than the measurements for the remainder of the test duration. The titanium witness plate temperature predictions were slightly lower than the measurements. The corresponding graph of the difference of predictions and measurements as a function of time for the three measurement locations is shown in Fig 17a. For Tc_1, predictions were higher than measurements up to 86 seconds with a maximum difference of 20.2°C in this time period. The predictions were then lower than the measurements for the rest of the test with a maximum absolute value difference of 30.2°C during this time period. The same patterns but with slightly lower differences were observed for Tc_2. For Ti_{cen} the difference between measurements and predictions varied between 0°C and 8.1°C. The ratio of the difference between measurement and prediction to the maximum measured temperature for Tc_1, Tc_2, and Ti_{cen} is provided in Fig. 17b. The difference for Tc_1 and Tc_2 varied between -7% and 4% during the test. The difference for Ti_{cen} varied between -5% and 0% during the test.

The same patterns were observed for tests 10 and 11 which were the other two tests with nominal 180 second long flame exposures.

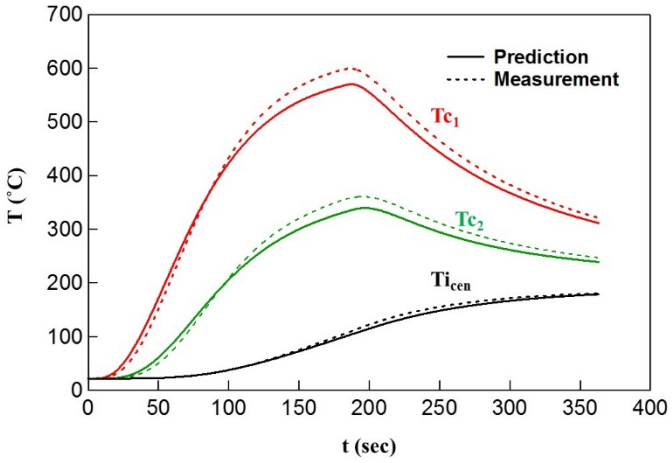

Figure 16. Comparison of predicted and measured temperatures for test 9

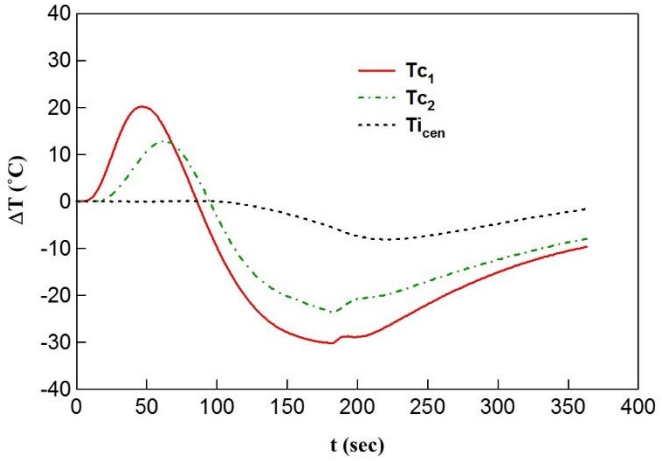

a)

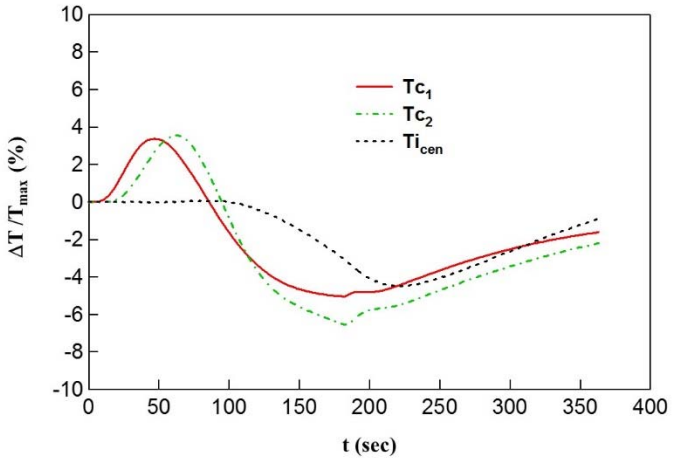

b)

Figure 17. Variation of difference between predicted and measured temperatures for test 9: a) absolute differences; b) percent differences

The temperature distributions for test 12, which was the test with 120 second flame exposure duration is provided in Fig. 18. The data shown are S_{avg}, Tc_1, Tc_2, Ti_{cen} , Ti_{edeg}, and Tc_3. The graph of the difference of numerical model predictions and measurements as a function of time for the three measurements locations (Tc_1, Tc_2, and Ti_{cen}) for this test is shown in Fig 19a. The observed trends were similar to trends for test 9. The ratio of the difference between measurement and prediction to the maximum measured temperature for Tc_1, Tc_2, and Ti_{cen} is provided in Fig. 19b. The difference for Tc_1 and Tc_2 was within ±5% during the test. The difference for Ti_{cen} varied between -4% to 0%. The temperature distributions for test 13, which was the test with 300 second flame exposure duration is provided in Fig. 20. Thermocouple Tc_2 was not operational for this test. The graph of the difference of numerical model predictions and measurements as a function of time for Tc_1 and Ti_{cen} for this test is shown in Fig 21a. Same general trends were observed as in test 9. The ratio of the difference between measurement and prediction to the maximum measured temperature for Tc_1 and Ti_{cen} is provided in Fig. 21b. The difference for Tc_1 was within ±5% during the test. The difference for Ti_{cen} varied between -3% to 0%.

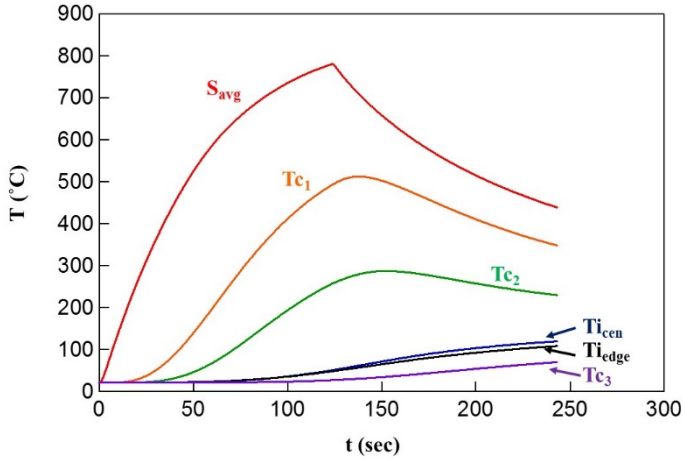

Figure 18. Test 12 temperature data

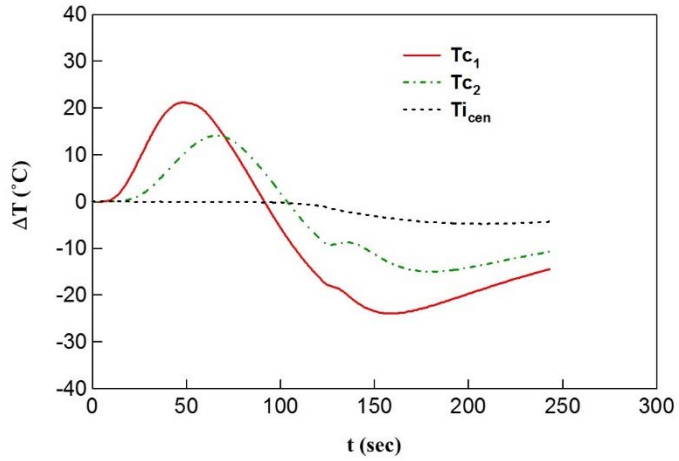

a)

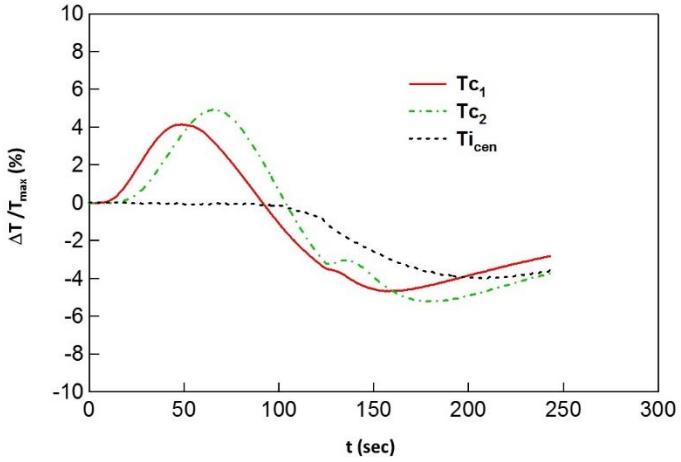

b)

Figure 19. Variation of difference between predicted and measured temperatures for test 12: a) absolute differences; b) percent differences

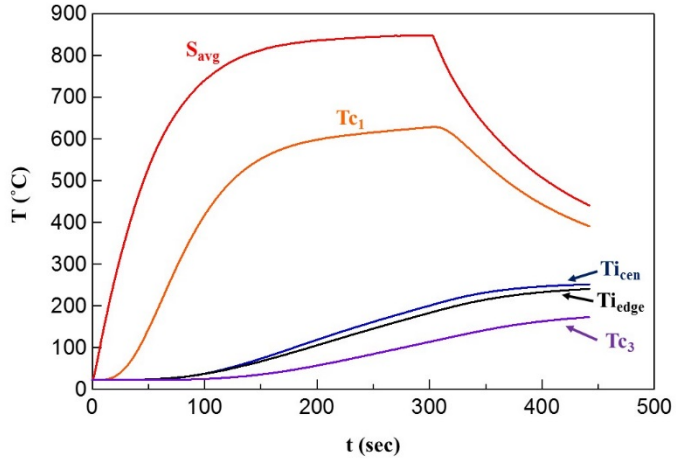

Figure 20. Test 13 temperature data

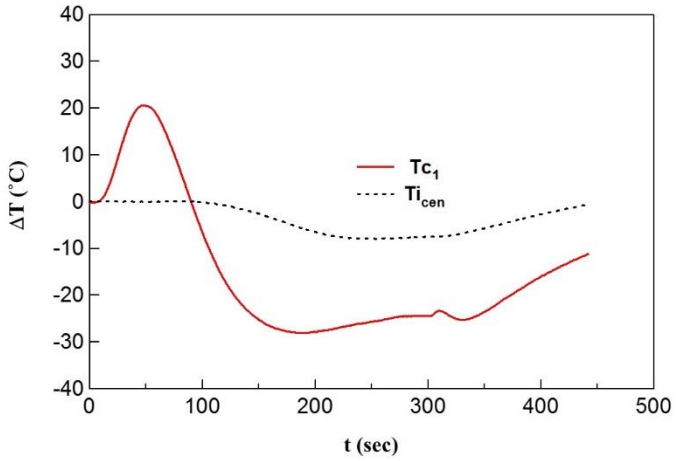

a)

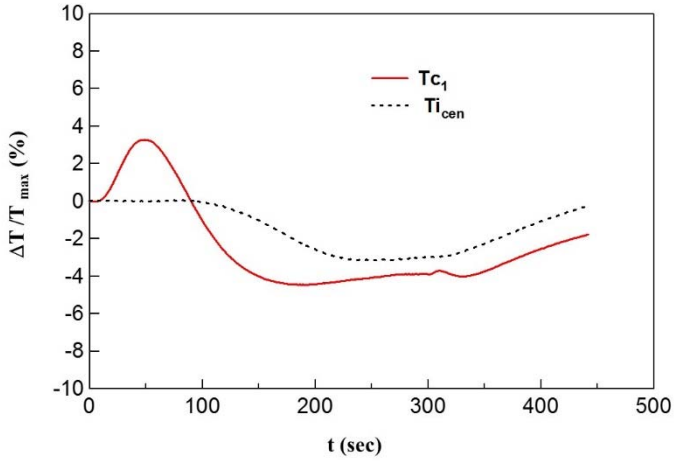

b)

Figure 21. Variation of difference between predicted and measured temperatures for test 13: a) absolute differences; b) percent differences

A tabulation of maximum absolute value difference and root mean square (RMS) difference between predictions and measurements for Tc_1, Tc_2 and Ti_{cen} are presented in Table 5. The RMS differences between predictions and measurements varied between 16.9°C and 21.0°C for Tc_1, between 10.5°C and 14.5°C for Tc_2, and between 2.8°C and 4.9°C for Ti_{cen}. The maximum absolute value difference varied between 23.9°C and 30.2°C for Tc_1, between 15°C and 23.6°C for Tc_2, and between 4.8°C and 8.1°C for Ti_{cen}. The corresponding ratio of RMS difference between predictions and measurements to the maximum measured temperatures for each quantity is presented in Table 6. The ratio of RMS difference to maximum temperature varied between 3.2% and 3.3% for Tc_1, between 3.6% and 3.9% for Tc_2, and between 1.6% and 2.2% for Ti_{cen}. The ratio of maximum difference between predictions and measurements to maximum temperature is not presented in the table, but varied between 4.5% and 5% for Tc_1, between 5.2% and 6.5% for Tc_2, and between 2.9% and 4.1% for Ti_{cen}.

As mentioned previously, neglecting the volumetric heat capacity of the foil thermocouples in the thermal analysis could explain some of the differences observed between predictions and measurements for

Tc_1 and Tc_2. But the close agreement between titanium plate temperature measurements and predictions, given all the possible sources of uncertainty in both the experimental data and numerical model, indicated that the THERMIC test assembly produced 1-D heat transfer in the center of test section, and was capable of providing reasonable test results that would match thermal model predictions.

Table 5. Deviations between predicted and measured temperatures at various thermocouple locations

Test Number	Tc_1	Tc_2	Ti_{cen}
	RMS/Max (°C)	RMS/Max (°C)	RMS/Max (°C)
9	19.7 / 30.2	14.5 / 23.6	4.4 / 8.1
10	19.2 / 28.3	13.1 / 20.5	3.8 / 7.1
11	19.2 / 29.2	13.5 / 21.9	4.0 / 7.6
12	16.9 / 23.9	10.5 / 15.0	2.8 / 4.8
13	21.0 / 28.0	----------	4.9 / 7.9

Table 6. Ratio of RMS deviation between predicted and measured temperatures to maximum temperature at various thermocouple locations

	RMS Deviation /Max Temperature (%)		
Test Number	Tc_1	Tc_2	Ti_{cen}
9	3.3	3.9	2
10	3.2	3.6	1.8
11	3.2	3.7	1.9
12	3.3	3.6	2.2
13	3.3	-------	1.6

Concluding Remarks

A simple transient thermal test, designated as THERMIC, was developed for evaluating the thermal performance of high-temperature flexible insulation materials in atmospheric pressure air. The test setup was inspired by the test assembly used for evaluating the performance of fire shelters and fire protective clothing provided in ISO 9151, but included some modifications to provide a suitable test bed for testing insulations. The test assembly consisted of a Meker burner supplied with propane gas, a rigid Inconel septum plate exposed to the flame, insulation test sample, and a titanium witness plate. Rigid and flexible ceramic insulations were used to minimize heat losses from the periphery of the test assembly. For this test assembly the ratio of the test insulation width to thickness was selected to be higher than ten so that the heat transfer in the center of the test assembly was nearly 1-D. Thermocouples installed on the septum and witness plates and inside the insulation test sample provided temperature measurements at various locations. The maximum Inconel septum plate temperature reached 780˚C to 850˚C for the various tests. Tests were conducted with flame exposure durations between 120 sec to 300 sec. An APA test sample with a density of 98.2 kg/m^3 was used for test assembly evaluation. The tests were repeatable as observed by close agreement between measured temperatures at various locations in the test assembly for tests with

similar flame exposure duration. A 1-D heat transfer model of the entire test assembly was used in conjunction with a measured specified temperature thermal boundary condition on the hot side and an adiabatic boundary condition on the cold side. The close agreement between measured and predicted temperatures on the titanium witness plate and inside the insulation test sample indicated that the test assembly can provide a 1-D thermal testing capability for evaluation of thermal performance of similar insulations.

References

1. ASTM Standard C 177, "Standard Test Method for Steady-State Heat Flux Measurements and Thermal Transmission Properties by Means of the Guarded-Hot-Plate Apparatus," 1996 Annual Book of ASTM Standards, Vol. 4.06, *Thermal Insulation, Environmental Acoustics*, 1996.

2. ASTM Standard C 518, "Standard Test Method for Steady-State Thermal Transmission Properties by Means of the Heat Flow Meter Apparatus," 1996 Annual Book of ASTM Standards, Vol. 4.06, *Thermal Insulation, Environmental Acoustics*, 1996.

3. Daryabeigi, K., Cunnington, G. R., and Knutson, J. R., "Combined Heat Transfer in High-Porosity High-Temperature Fibrous Insulations: Theory and Experimental Validation," *Journal of Thermophysics and Heat Transfer*, Vol. 25, No. 4, October–December 2011, pp. 536-546.

4. ASTM E1269-11, "Standard Test Method for Determining Specific Heat Capacity by Differential Scanning Calorimetry", ASTM International, West Conshohocken, PA, 2011. www.astm.org

5. "Protective Clothing against Heat and Flame - Determination of Heat Transmission on Exposure to Flame", ISO 9151:1995.

6. Fody, J. F., Daryabeigi, K., Bruce, W. E., Calomino, A. M., Wusk, M. E., and Wells, J. M., "Convective Heating Improvements for Emergency Fire Shelters (CHIEFS) _Second Generation Fire Shelter Concepts and Results from Full Scale Testing at NC State University, March 2016," NASA TM-2017-0219356, February 2017.

7. Daryabeigi, K., Knutson, J. R., and Cunnington, G. R., "Reducing Thermal Contact Resistance for Rigid Insulation Thermal Measurements," *Journal of Thermophysics and Heat Transfer*, Vol. 26, No. 1, January-March 2012, pp. 172-175.

8. Daryabeigi, K., "Design of High Temperature Multi-layer Insulation," Ph.D. Dissertation, University Of Virginia, May 2000.

9. Anderson, D. A., Tannehill, J. C., and Pletcher, R. H., *Computational Fluid Mechanics and Heat Transfer*, Hemisphere Publishing Corp., 1984.

10. Touloukian, Y. S., and Buyco, E. H., *Specific Heat, Nonmetallic Solids*, Vol. 5, Thermophysical Properties of Matter, IFI/Plenum, New York, 1970.

11. Williams, S. D, and Curry, D. M., "Thermal Protection Materials-Thermophysical Property Data," NASA RP-1289, December 1992.

REPORT DOCUMENTATION PAGE

Form Approved
OMB No. 0704-0188

1. REPORT DATE *(DD-MM-YYYY)*
1-02-2019

2. REPORT TYPE
Technical Memorandum

3. DATES COVERED *(From - To)*

4. TITLE AND SUBTITLE
A Simple Transient Thermal Test Assembly for Insulation Materials

5a. CONTRACT NUMBER

5b. GRANT NUMBER

5c. PROGRAM ELEMENT NUMBER

6. AUTHOR(S)
Daryabeigi, Kamran; Blosser, Max L.; Geouge, Wayne D.; Cheatwood, Jonathan S.

5d. PROJECT NUMBER

5e. TASK NUMBER

5f. WORK UNIT NUMBER
321991.02.23.01

7. PERFORMING ORGANIZATION NAME(S) AND ADDRESS(ES)
NASA Langley Research Center
Hampton, VA 23681-2199

8. PERFORMING ORGANIZATION REPORT NUMBER
L-20995

9. SPONSORING/MONITORING AGENCY NAME(S) AND ADDRESS(ES)
National Aeronautics and Space Administration
Washington, DC 20546-0001

10. SPONSOR/MONITOR'S ACRONYM(S)
NASA

11. SPONSOR/MONITOR'S REPORT NUMBER(S)
NASA-TM-2019-220249

12. DISTRIBUTION/AVAILABILITY STATEMENT
Unclassified-
Subject Category 34
Availability: NASA STI Program (757) 864-9658

13. SUPPLEMENTARY NOTES

14. ABSTRACT A simple transient thermal test was developed for evaluating the thermal performance of high-temperature flexible insulation materials in atmospheric pressure air. The test setup was inspired by the test assembly used for evaluating the performance of fire shelters and fire protective clothing. The heating source used was a burner supplied with propane gas that can generate relatively uniform heating over a wide area. The ratio of the in-plane width to thickness of the insulation test sample in the test assembly was selected to be greater than ten so that the heat transfer in the center of the test assembly was nearly one-dimensional. A rigid, thin Inconel plate was used as the septum plate directly exposed to the flame to provide a relatively uniform, known-temperature boundary condition for the test assembly, and to prevent convective heat transfer through the test insulation from the burner. The test sample, flexible alumina paper insulation, was placed between the Inconel plate and a thin titanium witness plate. The overall assembly was further insulated using a combination of rigid and flexible ceramic insulations to minimize heat losses from the periphery of the test assembly. Thermocouples installed on the septum and witness plates and inside the insulation test sample provided temperature measurements at various locations.

15. SUBJECT TERMS
High-temperature insulations; Thermal properties; Thermal testing

16. SECURITY CLASSIFICATION OF:			17. LIMITATION OF ABSTRACT	18. NUMBER OF PAGES	19a. NAME OF RESPONSIBLE PERSON
a. REPORT	b. ABSTRACT	c. THIS PAGE			STI Help Desk (email: help@sti.nasa.gov)
U	U	U	UU	28	19b. TELEPHONE NUMBER *(Include area code)* (757) 864-9658